MIRIS Pa α Galactic Plane Survey

Comparison with IPHAS H α in l = 96° - 116°

il-joong Kim

Korea Astronomy & Space Science Institute

Contents

1. Introduction
    1.1. Instrument MIRIS
    1.2. MIRIS Paα Data

2. MIPAPS: Comparison with IPHAS Hα in l = 96° - 116° (ApJS in 2018)
    2.1. Visual Inspection: Paα, Hα detections
    2.2. Photometric Results: E(B-V), Lyman continuum luminosity
    2.3. Morphological Results: E(B-V) map of Sh2-131

3. Future Plans for MIPAPS Data

1.1 Instrument MIRIS

◆ MIRIS (Multi-purpose IR Imaging System)

+ The primary payload of the Korean science and technology satellite 3, launched on 2013.

+ Specifications
  - Pixel scale: 51.6" × 51.6"
  - Field of view: 3.67° × 3.67°
  - Filters: I (1.05 μm), H (1.6 μm),
    Pa α line (1.875 μm),
    Pa α dual continuum (1.84 & 1.91 μm)

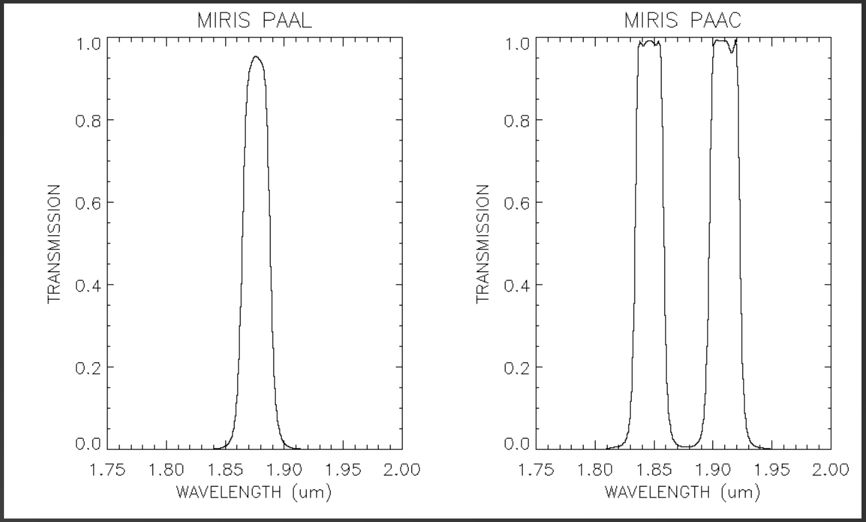

+ Main Goals
  - Cosmic Infrared Background (CIB) observation using I and H filters.
  - Pa α emission line survey of the whole Galactic plane using Pa α line filter.

1.2 MIRIS Paα Data

◆ MIRIS Paα Galactic Plane Survey (MIPAPS) data

+ Cover the whole plane (360°) with the width of $-3° < b < +3°$.

+ Total 235 fields with the average exposure of ~20 minutes (per filter).

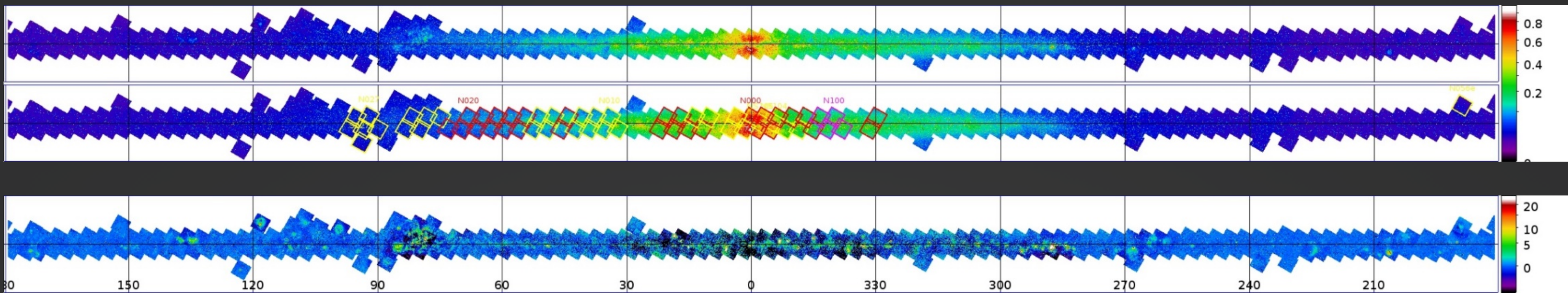

Top : Paα line filter (PAAL) image (mJy/arcsec^2)

Middle : Paα dual continuum filter (PAAC) image (mJy/arcsec^2)

Bottom : Paα emission line (PAAL-PAAC) image (10^{-19} W/m^2/arcsec^2)

+ The 1st data release on June, 2017. (http://miris.kasi.re.kr/miris/)

+ Need correction of edge-shadowing (by filter-wheel position offset) for $l = -30°$ to $95°$.

1.2 MIRIS Pa α Data

◆ Pointing observation data

+ Cover 19 targets (total 26 fields) located away from the Galactic plane.

- Nearby H II regions: M42, Rosette nebula, Lambda Orionis, California nebula, IC434, Barnard Loop, Gum nebula, Spica nebula, Zeta Ophiuchus.
- Star-forming clouds: Rho Ophiuchus, BFS11-B, Perseus cloud, NGC1579, Mon R2 cloud.
- Nearby galaxies: M31, SMC, LMC, NGC5457.
- North eclipse pole (NEP).

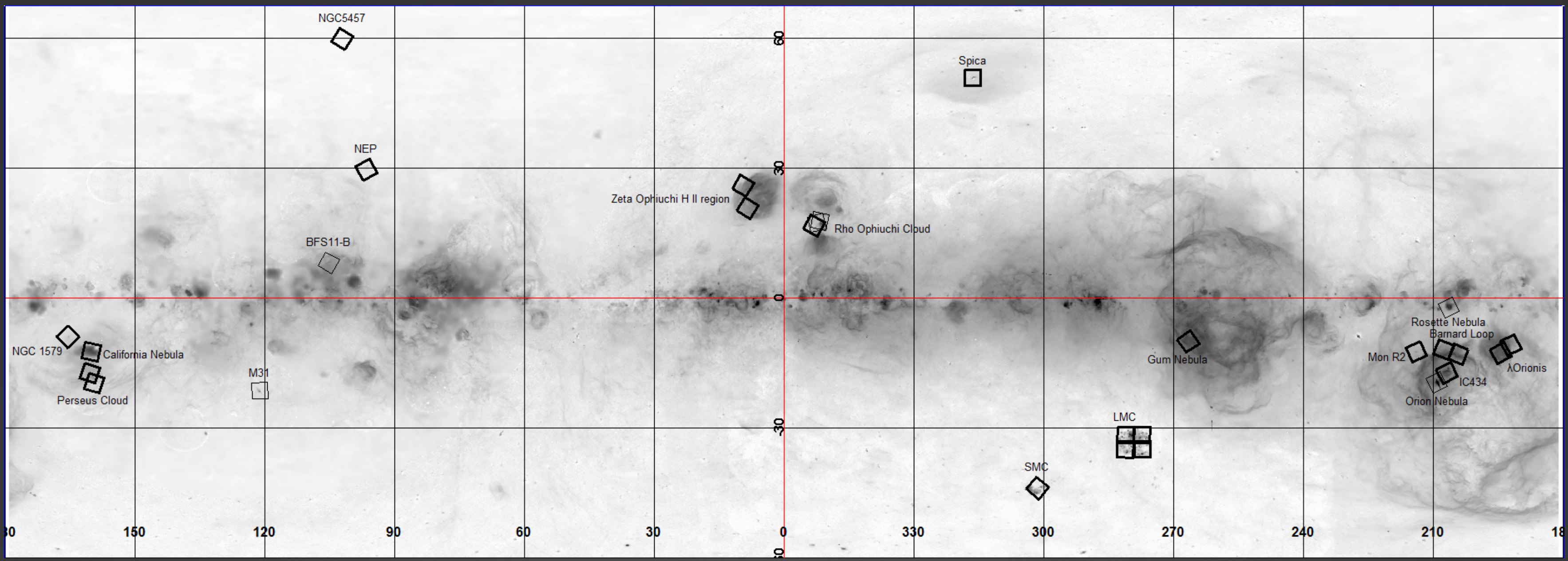

Positions of Pa α pointing observations on H α all sky map

2 MIPAPS: Comparison with IPHAS Hα in Cepheus

◆ The Cepheus region in outer Galaxy (l = 96° - 116°)

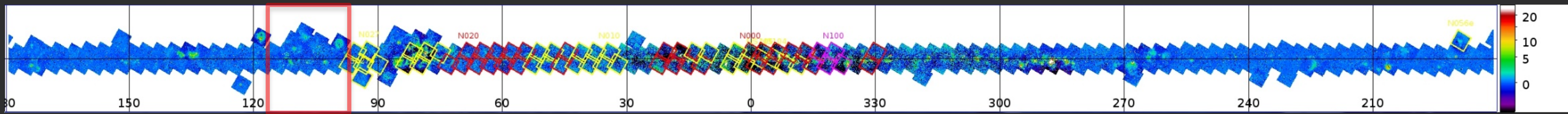

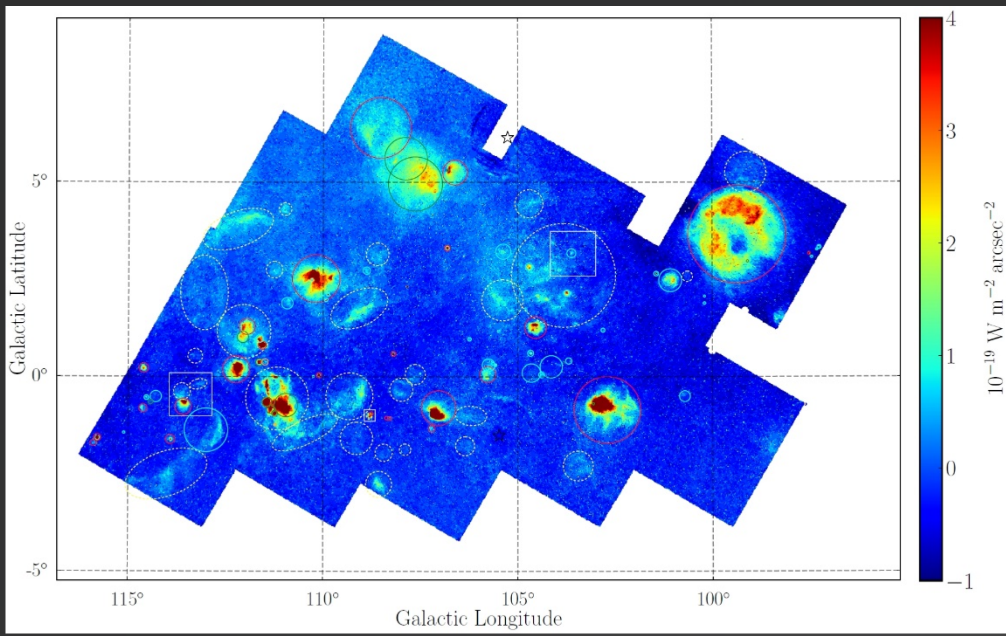

Continuum-subtracted MIPAPS Paα mosaic image

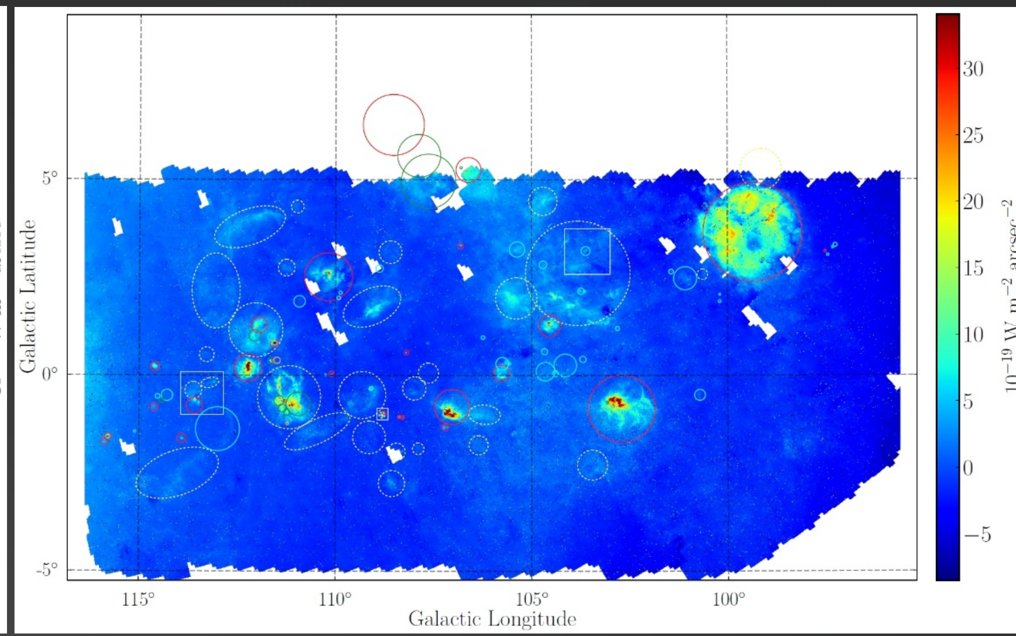

Continuum-subtracted IPHAS Hα mosaic image

+ WISE H II region sources (80): 27 Known, 39 Candidate, 12 Group, 2 Radio Quiet.

+ Unique MIPAPS Paα sources: 29 extended sources, 18 point-like sources.

2.1 Visual inspection

◆ WISE H II region sources (Anderson+ 2014)

+ Total 8399 sources based on MIR morphology: 22μm (heated dust) surrounded by 12μm (PAH).
+ Known: hydrogen recombination line (H α or RRL) detected.
+ Candidate: radio continuum detected, but no H α or RRL detected.
+ Group: spatially associated with known H II region complexes.
+ Radio Quiet: no counterparts at radio, H α and RRL; only MIR detected.

◆ Visual inspection for 212 WISE H II region sources in l = 96° – 116°

Summary of Visual Inspection for *WISE* H II Region Sources

Category	Number of Sources	MIPAPS Paα Detection			IPHAS Hα Detection				Paα and/or Hα Detection
		Yes		No	Yes		No	Not Observed	
"Known"	31	27	(87.1%)	4	27	(87.1%)	3	1	28
"Candidate"	71	39	(54.9%)	32	53	(74.6%)	18	0	54
"Group"	18	12	(66.7%)	6	16	(88.9%)	0	2	18
"Radio Quiet"	92	2	(2.2%)	90	18	(19.6%)	70	4	18
Total	212	80	(37.7%)	132	114	(53.8%)	91	7	118

+ Newly identified 90 sources as true (Known) H II regions (53 sources detected at Pa α).
+ Pa α > H α when E(B-V) >1.12 but, sources in l = 96° – 116° do not have heavy dust extinction.
+ MIPAPS Pa α data will be more useful in detecting H II regions toward the inner Galaxy.

2.1 Visual inspection

◆ Unique MIPAPS Paα sources

+ 29 extended sources: 13 have no known counterparts, but all have IPHAS Hα counterparts.

+ 18 Point-like sources: 3 PNe, 15 emission-line stars (including 6 WRs, 2 Herbig ABs).

MIPAPS Paα Extended Sources

ID	MIPAPS Name	Radius (arcsec)	Position Angle (deg)	Corresponding Known H II Region
MPE01	G099.14+05.26	1900	...	...
MPE02	G100.64+02.58	485	...	...
MPE03	G103.45−02.29	1380	...	GAL 103.39−02.28
MPE04	G103.82+02.61	4800	...	Sh2-134
MPE05	G104.71+04.45	1300	...	LBN 494
MPE06	G105.39+01.97	1900	...	[C51] 93
MPE07	G106.20−01.00	1460; 890	85	LBN 506
MPE08	G106.35−01.78	880	...	...
MPE09	G107.63+00.06	930	...	...
MPE10	G107.89−01.87	530	...	...
MPE11	G107.99−00.33	1070	...	LBN 513; Du 53; BFS 12; BFS 13
MPE12	G108.44−01.95	800	...	...
MPE13	G108.57−02.76	1200	...	Sh2-151
MPE14	G108.60+03.15	1050	...	...
MPE15	G108.81−01.01	270	...	Sh2-153
MPE16	G109.07+01.76	2800; 1640	115	Sh2-154
MPE17	G109.14−01.58	1500	...	Du 54
MPE18	G109.32−00.50	2170	...	Du 55
MPE19	G110.46−01.43	3275; 1100	115	...
MPE20	G110.97+04.31	580	...	...
MPE21	G111.18−00.56	2900	...	Sh2-157
MPE22	G111.25+02.75	770	...	...
MPE23	G112.03+01.16	2480	...	Sh2-161
MPE24	G112.19+03.79	3410; 1630	110	Sh2-160
MPE25	G113.05+02.16	3450; 2200	0	Du 56; Du 57
MPE26	G113.20−00.19	830; 450	103	...
MPE27	G113.28+00.53	680	...	...
MPE28	G113.62−00.38	780	...	...
MPE29	G114.02−02.50	3950; 2050	110	Du 58; Du 59

MIPAPS Paα Point-like Sources

ID	MIPAPS Name	Corresponding Known Object (Type)	IPHAS Hα Detection[a]
MPP01	G097.98−01.03	MWC 645 (emission-line star)	Y
MPP02	G098.26+04.91	PN K 3-60 (planetary nebula)	Y
MPP03	G099.21−01.18	AS 481 (emission-line star)	Y
MPP04	G099.53+04.40	HD 239712 (emission-line star)	Y
MPP05	G102.66+01.39	WR 151 (Wolf-Rayet star)	Y
MPP06	G102.78−00.65	WR 153 (Wolf-Rayet star)	Y
MPP07	G103.85−01.18	WR 154 (Wolf-Rayet star)	Y
MPP08	G104.11+01.00	PN Bl 2-1 (planetary nebula)	Y
MPP09	G105.32−01.29	WR 155 (Wolf-Rayet star)	Y
MPP10	G106.39+03.09	V669 Cep (emission-line star)	Y(P+D)
MPP11	G107.34+04.28	AS 492 (emission-line star)	No data
MPP12	G107.51+00.09	EM* GGR 102 (emission-line star)	Y(P+D)
MPP13	G107.67+01.40	MWC 657 (emission-line star)	Y
MPP14	G107.84+02.32	NGC 7354 (planetary nebula)	Y
MPP15	G109.82+00.92	WR 156 (Wolf-Rayet star)	No data
MPP16	G110.90+01.90	AS 505 (Herbig Ae/Be star)	Y
MPP17	G111.33−00.24	WR 157 (Wolf-Rayet star)	Y
MPP18	G111.73+00.04	MWC 1080 (Herbig Ae/Be star)	Y(P+D)

※ Three emission-line stars have diffuse IPHAS Hα features surrounding the point sources.

2.1 Visual inspection

◆ Three representative regions for visual inspection

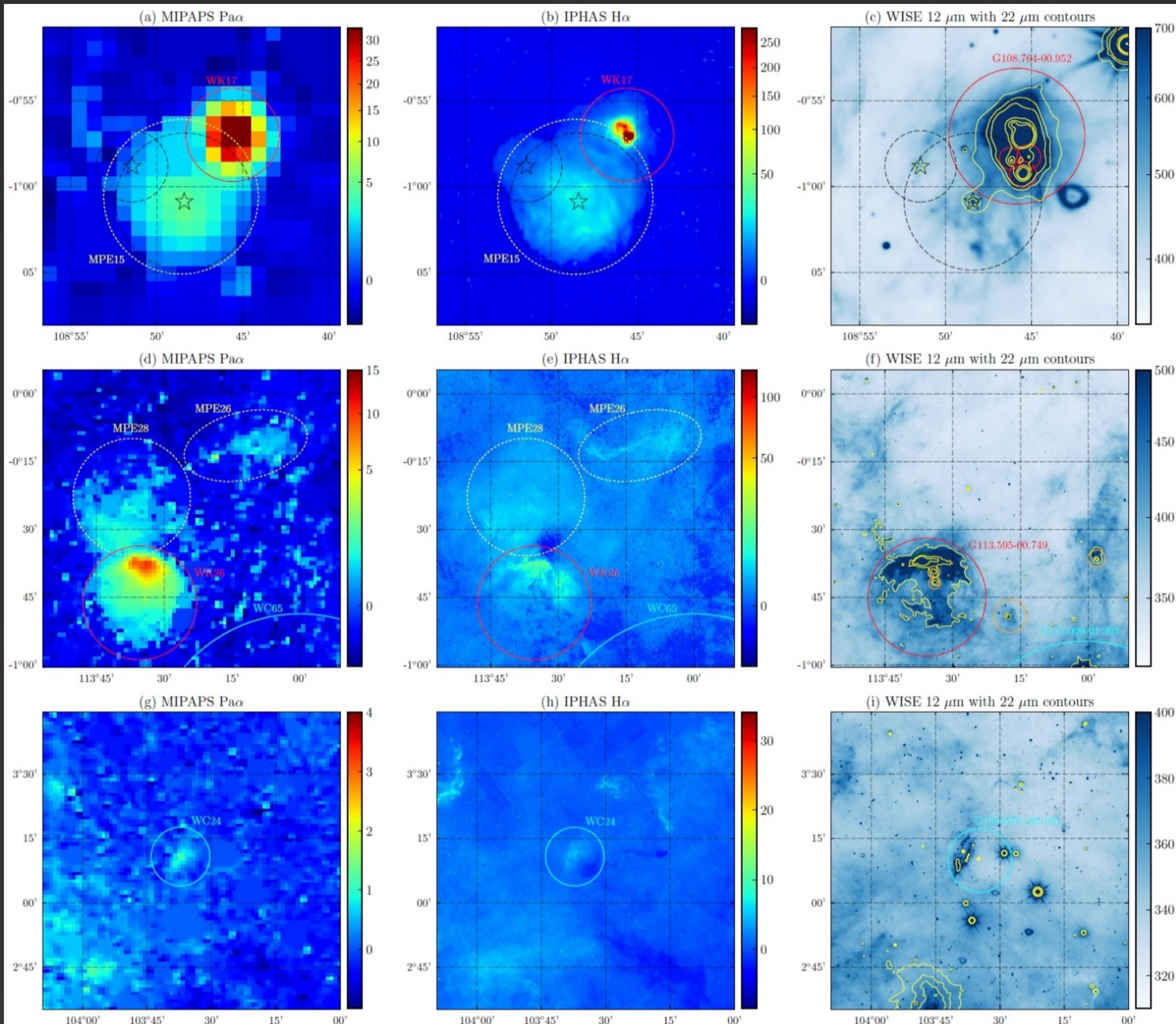

Left : MIPAPS Pa α

Center : IPHAS H α

Right : WISE 12 μm (22 μm contours)

WISE H II region sources

Known

Candidate

Radio Quiet

MIPAPS Pa α extended sources

Photometric Results

◆ E(B-V) estimation for 78 H II regions (or candidates)

+ Photometry of total Pa α and H α fluxes for 62 WISE H II region sources (22 Known, 30 Candidate, 9 Group, 1 Radio Quiet) and 16 MIPAPS Pa α extended sources.

+ Estimation of E(B-V) by comparing the observed fluxes with case B hydrogen recombination spectrum (Draine 2011).

WISE H II Region Sources: "Known"

ID	*WISE* Name	MIPAPS Name	Radius (arcsec)	Visual Inspection of Detection		Paα Total Flux (10^{-14} W m^{-2})	Hα Total Flux (10^{-14} W m^{-2})	*E*(*B*−*V*) (mag)
				Paα[a] (Stellar Residual Overlap)[b]	Hα[a]			
WK01	G097.515+03.173	G097.51+03.17	135	Y (partially)	Y	2.79 ± 0.03	1.46 ± 0.01	1.46 ± 0.01
WK02	G097.528+03.184	···	···	N (N)	Y	···	···	···
WK03	G099.484+03.801	G099.36+03.66	4535	Y (partially)	Y	1166.30 ± 1.62	6705.15 ± 3.14	0.20 ± 0.00
WK04	G102.877−00.695	G102.70−00.85	3085	Y (partially)	Y	375.57 ± 1.01	1385.85 ± 0.62	0.44 ± 0.00
WK05	G104.546+01.255	G104.54+01.27	1000	Y (partially)	Y	31.32 ± 0.31	93.50 ± 0.12	0.55 ± 0.01
WK06	G105.779+00.048	G105.77+00.06	740	Y (partially)	Y	14.18 ± 0.22	56.81 ± 0.09	0.39 ± 0.01
WK07	G106.605+05.252	G106.61+05.25	1145	Y (partially)	Yp	40.32 ± 0.37	···	···
WK08	G106.809+03.310	G106.81+03.31	260	Y (N)	Y	3.02 ± 0.06	2.49 ± 0.01	1.22 ± 0.01
WK09	G107.034−00.801	G107.03−00.80	1600	Y (partially)	Y	135.36 ± 0.47	502.16 ± 0.29	0.43 ± 0.00
WK10	G107.209−01.334	G107.21−01.33	300	Y (partially)	Y	1.34 ± 0.07	5.97 ± 0.02	0.34 ± 0.03
WK11	G108.191+00.586	G108.19+00.59	230	Y (N)	Y	10.66 ± 0.07	3.06 ± 0.02	1.77 ± 0.00
WK12	G108.273−01.066	G108.28−01.07	160	Y (largely)	Y	···	···	···
WK13	G108.375−01.056	G108.37−01.06	170	Y (largely)	Y	···	···	···
WK14	G108.503+06.356	G108.52+06.40	2800	Y (partially)	No data	127.56 ± 0.76	···	···
WK15	G108.752−00.972	···	···	N (N)	N	···	···	···
WK16	G108.758−00.989	···	···	N (N)	N	···	···	···
WK17	G108.764−00.952	G108.76−00.95	163	Y (partially)	Y	10.74 ± 0.08	13.37 ± 0.02	1.00 ± 0.00
WK18	G108.770−00.974	···	···	N (N)	N	···	···	···
WK19	G110.099+00.042	G110.10+00.04	250	Y (N)	Y	16.41 ± 0.06	16.49 ± 0.01	1.12 ± 0.00
WK20	G110.211+02.616	G110.18+02.52	2200	Y (partially)	Y	227.14 ± 0.60	290.04 ± 0.49	0.99 ± 0.00
WK21	G111.286−00.660	G111.29−00.66	165	Y (N)	Y	6.56 ± 0.17	13.66 ± 0.05	0.74 ± 0.01
WK22	G111.558+00.804	G111.56+00.81	375	Y (partially)	Y	113.36 ± 0.19	75.80 ± 0.06	1.33 ± 0.00
WK23	G111.612+00.371	G111.61+00.37	64	Y (partially)	Y	···	···	···
WK24	G111.946+01.336	G111.95+01.29	740	Y (partially)	Y	25.43 ± 0.23	61.04 ± 0.12	0.66 ± 0.00
WK25	G112.212+00.229	G112.23+00.19	1250	Y (partially)	Y	107.00 ± 0.40	407.68 ± 0.29	0.42 ± 0.00
WK26	G113.595−00.749	G113.59−00.77	755	Y (partially)	Y	24.87 ± 0.21	23.27 ± 0.07	1.15 ± 0.00
WK27	G113.900−01.613	G113.92−01.61	425	Y (N)	Y	3.22 ± 0.11	6.02 ± 0.03	0.79 ± 0.02
WK28	G114.626+00.219	G114.60+00.22	435	Y (partially)	Y	6.69 ± 0.14	17.75 ± 0.02	0.61 ± 0.01
WK29	G114.605−00.801	G114.62−00.81	372	Y (partially)	Y	3.17 ± 0.08	5.49 ± 0.02	0.83 ± 0.01
WK30	G115.785−01.561	G115.79−01.57	326	Y (partially)	Y	12.85 ± 0.11	23.48 ± 0.02	0.80 ± 0.00
WK31	G115.885−01.707	G115.89−01.71	285	Y (N)	Y	1.04 ± 0.11	2.57 ± 0.02	0.65 ± 0.05

2.2 Photometric Results

◆ Pa_α - H_α E(B-V)

+ Negative and positive correlation with angular size and distance, respectively.
+ WC51 with high E(B-V) and small distance could be a young ultracompact H II region.

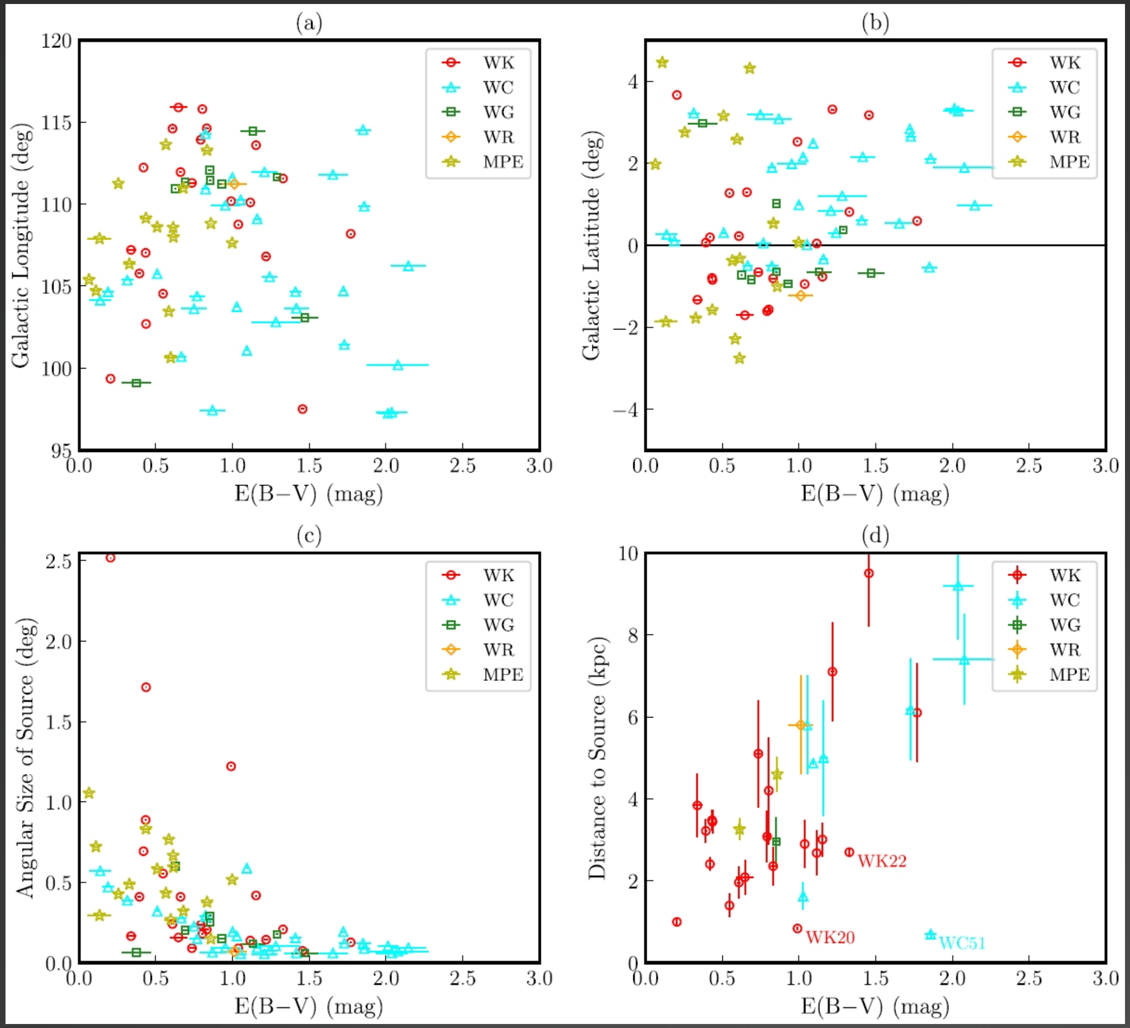

E(B-V) vs.

(a) Galactic longitude

(b) Galactic latitude

(c) Angular size of source

(d) Distance to source

2.2 Photometric Results

◆ Comparison of Pa α - H α E(B-V) with other E(B-V)

+ Foster & Brunt (2015): obtained E(B-V) for 103 H II regions from photometry of discrete point stars associated with the H II regions.

+ Good agreement within ~0.4 mag.

+ But, Pa α - H α E(B-V) are systematically lower.

: offset of 0.10-0.23 mag (T=5,000-20,000 K).

+ Pa α - H α E(B-V) were derived from photometry of extended emissions from ionized hydrogen gas.

→ Dust scattering contributes 0.10-0.23 mag to Pa α - H α E(B-V) from extended sources.

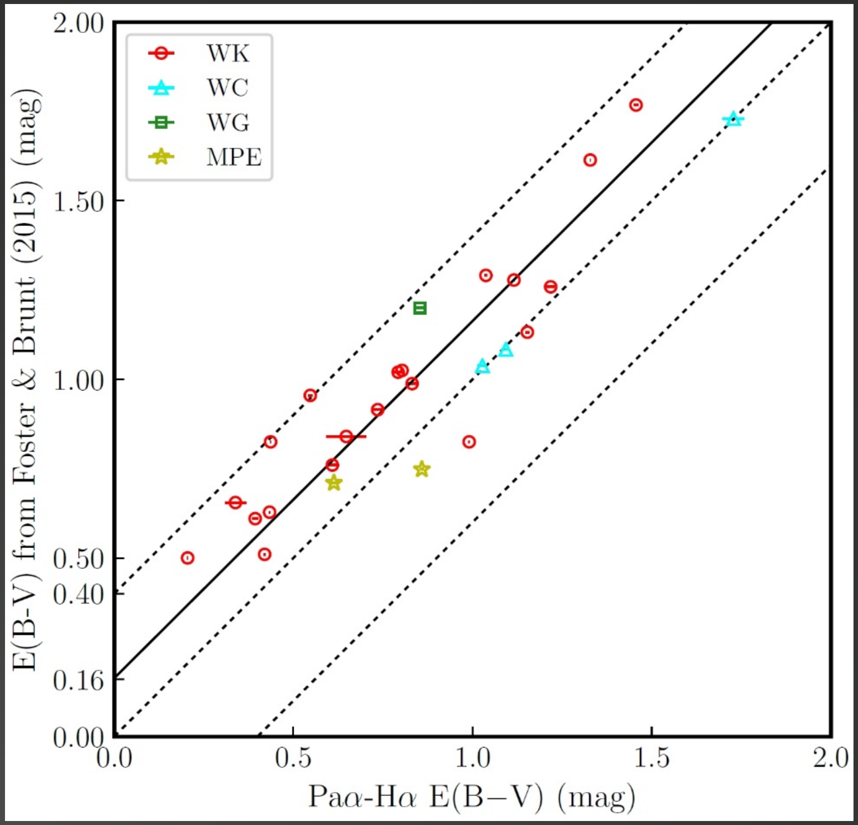

Pa α - H α E(B-V) vs.

E(B-V) from Foster and Brunt (2015)

2.2 Photometric Results

◆ Estimation of total Lyman continuum (Lyc) luminosity for H II regions

+ Obtain reddening-corrected Pa α (or H α) total flux using the observed fluxes and E(B-V).

+ Estimation of total Lyc luminosity emitted from ionizing stars (as a function of distance) by comparing with case B hydrogen recombination spectrum (Draine 2011).

+ Spectral types corresponding to the Lyc luminosities (Martins+ 2005).

→ can constrain either distance or ionizing spectral type for H II regions, if we know the other one.

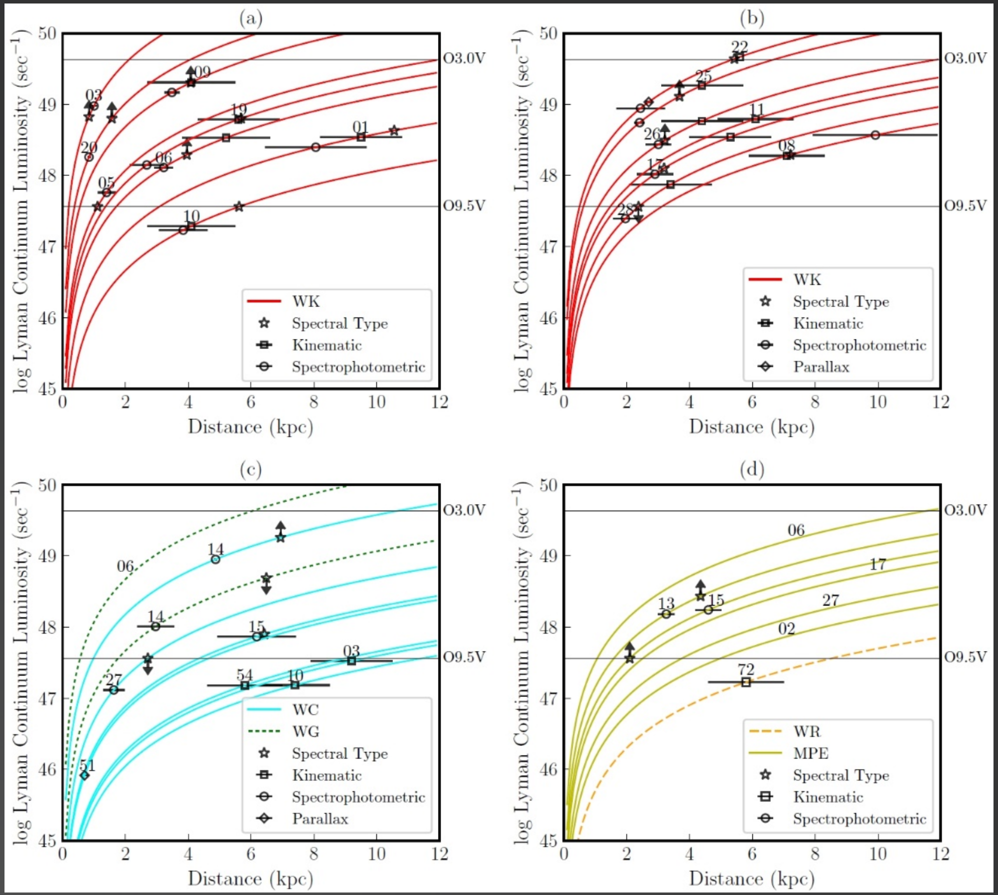

Ex) WK22 (known as Sh2-158)

Parallax distance: 2.7 kpc

Spectrophotometric distance: 2.44 kpc

Kinematic distance: 5.6 kpc

Ionizing stars: O3V and O9V (Russeil+ 2007)

O7V (Lynds & O' Neil 1986)

2.3 Morphological Results

◆ E(B-V) map of Sh2-131

+ NW part: filamentary features with high E(B-V), which reveal foreground dust clouds.
+ SE part: negative E(B-V) along the outer rim, indicating $H\alpha$ excess.

→ due to dust-scattering halo surrounding H II regions (Seon & Witt 2012).

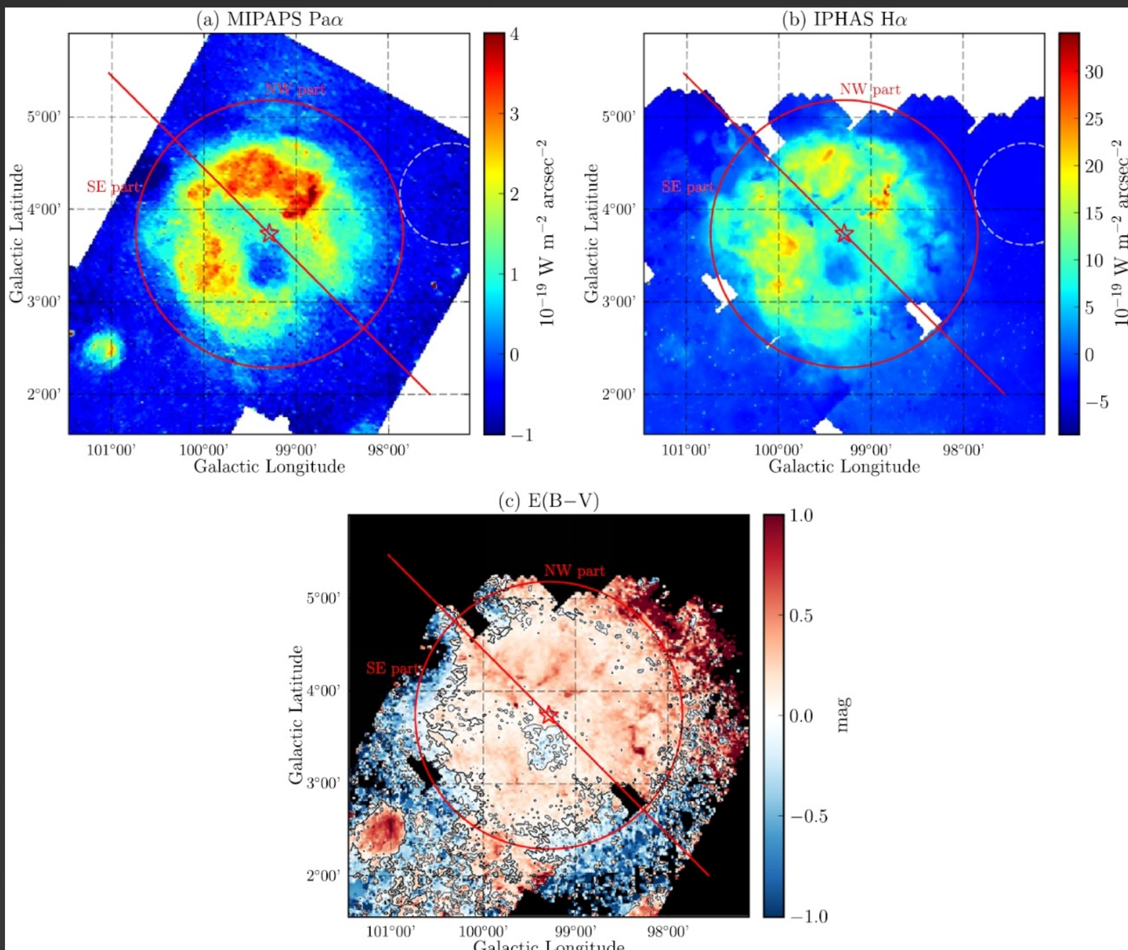

<u>Upper left</u> : MIPAPS Pa α

<u>Upper right</u> : IPHAS H α

<u>Lower</u> : E(B-V)

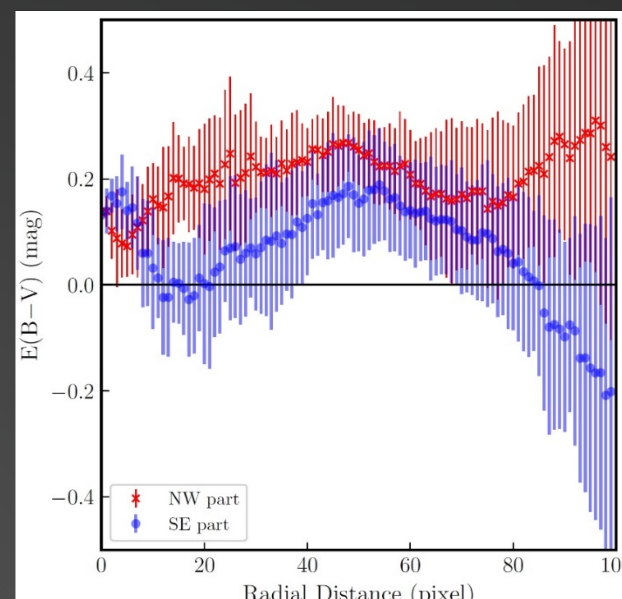

2

MIPAPS: Comparison with IPHAS Hα in Cepheus

◆ Summary

1. Visual Inspection

+ Newly identified 90 H II region candidates as definite H II regions (53 detected at Paα).

+ Additional 29 extended and 18 point-like sources at Paα.

2. Photometric Results

+ Paα - Hα E(B-V): under-estimation of 0.10-0.23 mag by dust scattering effect.

+ Total Lyman continuum luminosity: constrains distance & ionizing spectral type for H II regions.

3. Morphological Results

+ High E(B-V) filamentary features: reveal foreground dust clouds.

+ Negative E(B-V) regions: detection of Hα excess by dust scattering effect.

3

Future Plans for MIPAPS Data

◆ Analysis for data quality and scientific potential

+ The 1st region: Cepheus in outer Galaxy ($l = 96° - 116°$) → published in 2018.
+ The 2nd region: Carina in inner Galaxy ($l = 276° - 296°$) → to be submitted in 2019.

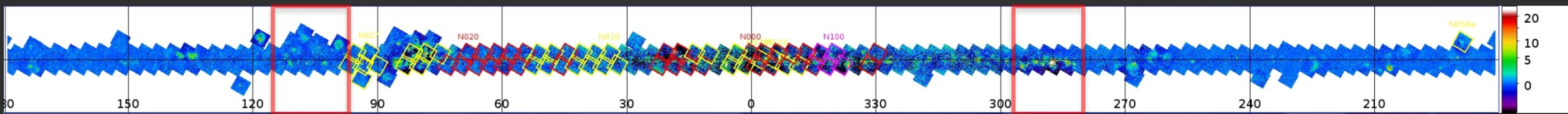

◆ Correction of edge-shadowing effects for $l = -30°$ to $95°$

+ Check the status of affected data.
+ Crop or correct for 602 orbit data by using stray light simulations.

◆ Final goals

+ The whole plane MIPAPS Paα image.
+ The whole plane MIPAPS Paα source catalog.